Available online at www.sciencedirect.com
ScienceDirect
Journal of Solid State Chemistry 179 (2006) 3997–4002
JOURNAL OF SOLID STATE CHEMISTRY
www.elsevier.com/locate/jssc

Photoluminescence: A probe for short, medium and long-range self-organization order in $ZrTiO_4$ oxide

Poty R. de Lucena[a,*], Edson Roberto Leite[a], Fenelon M. Pontes[b], Elson Longo[c], Paulo S. Pizani[d], José Arana Varela[c]

[a]*Departamento de Química, Universidade Federal de São Carlos-UFSCar, Caixa Postal 676, 13560-905 São Carlos, SP, Brazil*
[b]*Faculdade de Ciências, UNESP, Bauru, SP., Brazil*
[c]*Instituto de Química, UNESP, Araraquara, SP., Brazil*
[d]*Departamento de Física, Universidade Federal de São Carlos-UFSCar, São Carlos, SP, Brazil*

Received 18 April 2006; received in revised form 3 September 2006; accepted 10 September 2006
Available online 17 September 2006

Abstract

Photoluminescent disordered $ZrTiO_4$ powders were obtained by the polymeric precursor soft-chemical method. This oxide system (ordered and disordered) was characterized by photoluminescence, Raman spectroscopy, X-ray diffraction, differential scanning calorimetry and UV–vis absorption experiments. The UV absorption tail formation in the disordered oxides was related to the diminution of optical band gap. In the disordered phase, this oxide displayed broad band photoluminescence caused by change in coordination number of titanium and zirconium with oxygen atoms. The gap decreased from 3.09 eV in crystalline oxide to 2.16 eV in disordered oxide. The crystalline oxide presented an orthorhombic α-PbO_2-type structure in which Zr^{4+} and Ti^{4+} were randomly distributed in octahedral coordination polyhedra with oxygen atoms. The amorphous–crystalline transition occurred at almost 700 °C, at which point the photoluminescence vanished. The Raman peak at close to 80–200 cm^{-1} indicated the presence of locally ordered Ti–O_n and Zr–O_n polyhedra in disordered photoluminescent oxides.

Keywords: $ZrTiO_4$; Photoluminescence; Polymeric precursor method; Order–disorder level

1. Introduction

The electronic industry's growing demand for novel materials drives technological research into materials with new and more efficient properties. Since the discovery of electronic properties in amorphous silicon and other condensed systems, the discussion about how atoms and molecules originate periodically structured materials has taken a new turn. In 1972, Lines calculated the thermodynamic quantities of a glass-like structure in disordered material and proved the existence of ferroelectricity in this system [1]. The development of new techniques to produce covalent solids based on soft synthesis at low temperatures created new prospects in this area, mainly thanks to the possibility of producing periodically disordered structures with preferentially oriented atoms, creating controlled systems in templates, zeolites, oxalates, polymers or complexes environments for metallic ions, resulting in new oxides with new morphologies and surprising properties.

Chemical preparation methods, especially co-precipitation, sol–gel synthesis and polymeric routes, offer advantages over traditional physical reactions of component oxides in terms of higher purity and greater homogeneity, as well as the possibility of producing oxide systems at various self-organization levels by controlling the heat treatment of an initial precursor [2,3]. The polymeric precursor method (PPM) [4–6] has been used to synthesize photoluminescent covalent oxides with disordered structures. This method (PPM) is associated with the formation of a metallic complex using a hydroxycarboxylic acid such as citric acid. Polymerization is promoted by heating the complex in the presence of a polyhydroxy alcohol such as ethylene glycol [7]. A homogeneous resin, the polymeric

*Corresponding author. Fax: +55 16 3351 5215.
E-mail address: poty@liec.ufscar.br (P.R. de Lucena).

0022-4596/$ - see front matter © 2006 Elsevier Inc. All rights reserved.
doi:10.1016/j.jssc.2006.09.010

precursor, is produced, in which the metal ions are uniformly distributed within the organic matrix [8].

The discovery that non-periodic (disordered) covalent oxides produce visible photoluminescence at room temperature opened up a new round of discussions regarding this electronic phenomenon [9]. Orhan et al. [10,11] attributed photoluminescent behavior in disordered materials to the presence of new electronic levels between the valence (VB) and conduction bands (CB) of various covalent titanate and tungstate [12–14]. X-ray appearance near-edge structure (XANES) experimental results on photoluminescent disordered $SrTiO_3$ and $PbTiO_3$ that had been synthesized by the PPM and whose thermal treatment had been done at temperatures inferior to their crystallization threshold pointed out the coexistence of two types of environments for the titanium, namely, five-fold coordination $Ti–O_5$ (square-base pyramid) and six-fold $Ti–O_6$ coordination (octahedron) [15].

$ZrTiO_4$ (ZT) is widely used in the electronic industry, where there is a strong demand for high-performance dielectric materials [16]. This oxide also has numerous applications as a catalyst in oxidation reactions [17]. ZT displays an α-PbO_2 orthorhombic structure with a random distribution of the Zr^{4+} and Ti^{4+} cations at equivalent octahedral sites. The oxygen atoms in this oxide system form a compact hexagonal arrangement, with Ti^{4+} and Zr^{4+} cations occupying, in equiatomic amounts, the octahedral sites in the lattice, where each metal is coordinated by six oxygens [18]. In this work, oxides treated at temperatures below and above the crystallization temperature (700 °C) are classified, respectively, as disordered and ordered oxides.

According to Xu and coworkers [19], based on the analysis of Zr–O and Ti–O bonds by XANES experiments, the structural crystallization of ZT at 700 °C from an amorphous chemical precursor (dry-gel) is accompanied by a change in the chemical coordination of titanium, from five-fold (TiO_5) to six-fold coordination (TiO_6) and zirconium from seven-fold (ZrO_7) to six-fold coordination (ZrO_6), toward orthorhombic phase formation.

In this article, we report and discuss the structural and optical properties in the visible spectral region of the ZT powders obtained by soft-chemical method. As a consequence, the influence annealing temperature could also be investigated.

2. Experimental

Fig. 1 illustrates the preparation of disordered and ordered $ZrTiO_4$ by the PPM. The titanium and zirconium citrates were prepared from titanium isopropoxide [Riedel-de-Haën] and zirconium *n*-propoxide [Quimex], respectively, by dissolution of them in an aqueous solution of citric acid (CA) with 3:1 relation of CA:metal. The polyetherification was promoted by increase of temperature to 100 °C, by water evaporation.

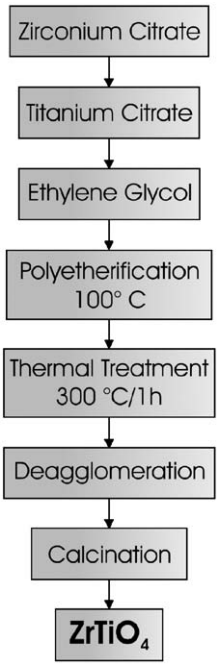

Fig. 1. Schematic flow chart for polymeric precursor processing of ordered and disordered $ZrTiO_4$ powder.

After the water evaporation, the polymeric resin was heat-treated at 300 °C for 1 h in a static atmosphere, leading to the partial decomposition of the polymeric gel and the formation of an expanded resin composed of partially pyrolyzed material. The product of this primary heat treatment (disordered oxide precursor) was deagglomerated and grounded in a porcelain mortar until it passed through a 100-mesh sieve. This oxide precursor was calcined at 400, 500, 600 and 700 °C in a conventional furnace and also at 650, 660, 670 and 680 in DSC furnace to examine the structural organization of the ZT oxide in function of the thermal treatment temperatures, at a heating rate of 10 °C min^{-1}. Differential calorimetry experiments (DSC) were made with a DSC Pegassus 404 Netzsch-Germany calorimeter with air atmosphere in a temperature range of 25–1000 °C.

The structural organization was evaluated by XRD, using a Rigaku DMax 2500 PC X-ray diffractometer with CuKα radiation ($\lambda = 1.5406$ Å) operating at room temperature. The data were collected in the 5°–75° 2θ range. ZT diffracted peak positions were confirmed with the joint cards pattern diffraction stand (JCPDS) no. 34-415.

The photoluminescence spectra were obtained at room temperature, using a U1000 Jobin–Yvon double monochromator coupled to a GaAs photomultiplier and a conventional photon counter. 488 nm Ar ion laser wavelengths were utilized, with the high power output at 180 mW.

For the UV diffuse reflectance analysis, we used a UV–vis NIR Cary 5G spectrometer operating in diffuse reflectance mode in the energy range of 300–800 nm. The Kubelka–Munk function was used to convert reflectance

measurements into equivalent absorption spectra using the reflectance of MgO as a reference [20]. The gap values were obtained by the Tauc method [21].

Raman measurements were taken with an RFS/100/S Bruker FT–Raman spectrometer equipped with a Nd:YAG laser in a fixed wavelength of 9394.6 cm^{-1} in the 100–1000 cm^{-1} spectral interval. The spectrometer's resolution was 4 cm^{-1} and laser power 50 mW.

3. Results and discussion

3.1. Phase formation

ZT displays two-phase transitions when cooled from higher temperature: from normal to incommensurate at 1250 °C and from incommensurate to commensurate at 850 °C [16,22]. The structure of ZT in each phase has a strong dependence with Zr and Ti ordering in octahedral positions [23]. The normal phase is ordered, and this behavior can be noted by the better definition of the Raman spectra peaks and by the presence of two satellite peaks in X-ray diffraction (XRD) patterns relative to superlattice reflections. With the disorganization of the structure in the incommensurate phase, Raman peaks become broader and the satellite peaks in XRD disappear [24]. The integral periodicity is recovered with commensurate phase formation.

Our work is based on the study of the local and periodic structure of ZT oxide obtained from precursor powders treated at temperatures below the temperature of crystallization (non-periodic condition), in contrast to the above-cited works.

Based on the XRD and DSC measurements, the formation of ZT ordered phase occurred at temperatures above 700 °C. The ordered oxide powders treated at 700 °C presented an orthorhombic ZT-type structure in the crystalline phase (JCPDS file number 34-415), and no secondary phases were detected by XRD (Fig. 2). The lattice parameters calculated for the ordered $ZrTiO_4$ by interplanar distance equations of the orthorhombic lattice were $a = 4.879$ Å, $b = 5.411$ Å and $c = 5.014$ Å. The amorphous precursor subjected to heat treatments at temperatures below 700 °C did not display a characteristic diffraction pattern of ZT crystalline structure. Only the crystalline ordered α-PbO_2 phase was attained when the temperature was increased to 700 °C. These results corroborate the crystallization temperature of the oxides determined in a previous study by DTA and XRD, which indicated a crystallization temperature of about 700 °C [25].

Fig. 3 depicts ZT XRD patterns of the powders treated in the 650–680 °C temperature interval, while the inset shows the DSC peak of ZT crystallization from amorphous precursor. As indicated by the exothermic peak in the DSC analysis, ZT presented crystllization peak at around 700 °C dividing the disordered and ordered phases. To evaluate the starting point of phase formation, the ZT powders were heat-treated at 650, 660, 670, and 680 °C in a DSC oven in alumina pans. The XRD patterns of the samples heated at these temperatures display undefined phase, with the presence of a few peaks with maximum intensity equal to $\frac{1}{10}$ of the crystalline 100% peak diffraction intensity in ordered samples (>700 °C), probably a noise of the XRD measure.

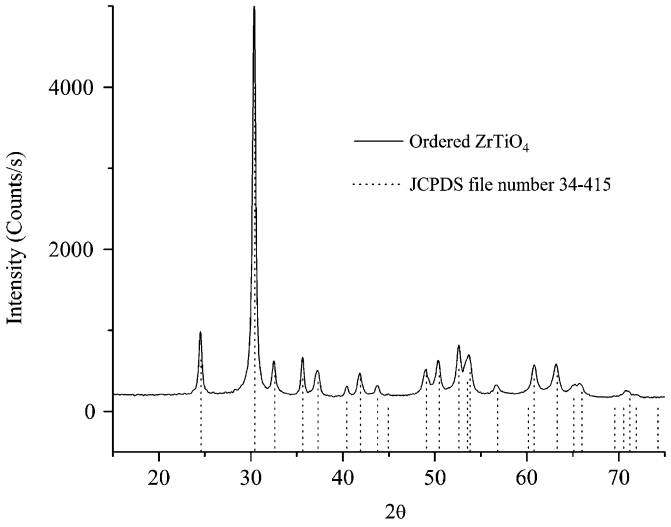

Fig. 2. $ZrTiO_4$ XRD pattern for powder heat-treated at 700 °C. The dashed lines indicate the position and relative intensity of orthorhombic 34-415 JCPDS card file diffraction peaks.

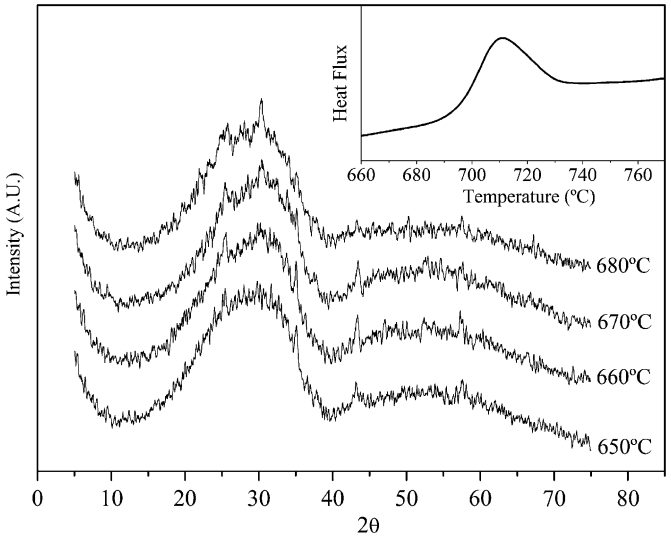

Fig. 3. XRD patterns for $ZrTiO_4$ powder in the 650–680 °C temperature interval. The inset shows the exothermic DSC peak relative to structural organization event from disordered to ordered phase.

3.2. Raman spectroscopy

In an ordered phase, Raman soft-modes are associated with atomic dislocations in a parallel (longitudinal mode, *LO*) and perpendicular (transversal mode, *TO*) direction to the direction of wave propagation in a lattice cell. These

dislocations can be detected by Raman spectroscopy not only in periodically ordered oxides but also in disordered oxides. Fig. 4 presents the Raman spectra for the ZT powder treated at 400, 500, 600 and 700 °C. In a study of ZT catalytic properties, Reddy et al. [26] described some characteristic Raman peaks of the ZT crystalline phase.

The representation for the Raman active normal modes (Γ_{RA}) in ZT with α-PbO_2 structure can be written using the following representations:

$$\Gamma_{RA} = 4A_g + 5B_{1g} + 4B_{2g} + 5B_{3g}. \quad (1)$$

The classification of each active mode of a ZT Raman spectrum is very difficult due to the structural conformation of this oxide. However, some previous works identified the ZT Raman peaks.

The observed peaks positions were compared with literature values reported for orthorhombic ZT [24,27,28] and are displayed in Table 1.

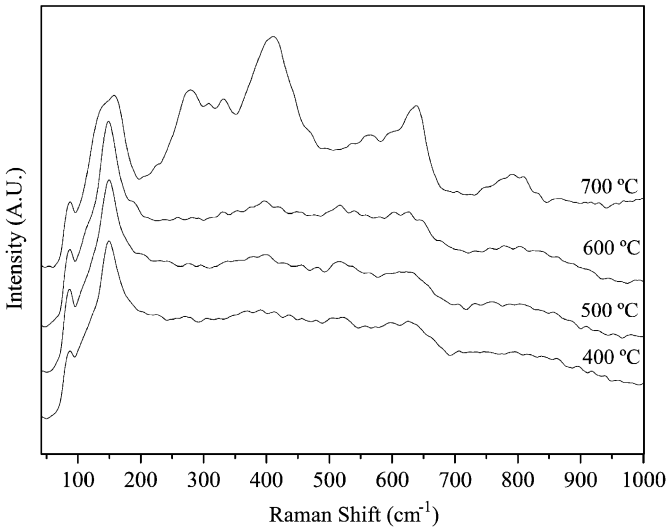

Fig. 4. Raman spectral dependence of the $ZrTiO_4$ oxide to the heat treatment temperature.

Table 1
Raman identified normal modes in crystalline $ZrTiO_4$

[24]	[27]	[28]	This study
—	—	—	85
131	124	—	131
160	154	—	160
—	258	260	—
273	269	290	276
327	331	320	333
—	394	—	—
407	415	400	411
—	537	—	—
579	590	580	566
—	626	—	603
637	646	640	637
—	—	—	768
792	795	800	802

In comparison to the literature results, the number and position of peaks of the Raman spectra (Fig. 4) show a minimal discrepancy. These fluctuations are related to different syntheses methodologies, in particular to the thermal treatment of ZT precursors. Raman results founded in the literature are based in ZT obtained from $ZrO_2 : TiO_2$ oxide mixture in temperatures above 1400 °C.

Despite of the low calcination treatment temperature of ZT, the Raman spectra display some vibrational events in disordered phases (300, 400, 500 and 600 °C heat treatment temperature), with vibrational events in the region of 80–200 cm^{-1}. These peaks are related to the short-range interaction of the Ti–O_n and Zr–O_n bonds in a previous event of periodic phase organization. This short-range interaction was able to produce broad Raman peaks in 80–200 cm^{-1}, but was unable to define the diffraction pattern characteristic of crystalline ZT.

According to Petzelt and coworkers [29], the 84 cm^{-1} mode displays the TO_1 transversal mode relating to the inclination of the Ti–O_n polyhedrons in disordered and ordered oxides. Thus, in our system, in the disordered condition, the ZT oxides probably presented a local order of Ti–O_n polyhedrons with variable coordination number (n).

As described in the previous section, the oxide presented only crystalline phase after being heat-treated above 700 °C. Hence, the Raman peaks in the oxide treated at 700 °C are characteristic of the orthorhombic long-range structure of ZT.

3.3. UV tail absorption

UV–visible diffuse reflectance spectroscopy is a useful spectroscopic technique that probes the electronic structure and domain size of transition metal oxides. The position of the absorption edge is sensitive to the bonding between metal oxide polyhedra. According to Wood and Tauc [21], the band gap in the high-energy region of the absorbance spectra of semiconductor oxides is related to oxide absorbance and photon energy by

$$h\nu\alpha = (h\nu - E_g^{opt})^2, \quad (2)$$

where α is absorbance (K/S in Kubelka–Munck conversion), h is Plank's constant, ν is the frequency and E_g^{opt} is the optical band gap. The band gap is obtained by fitting of linear region of curves illustrated in Fig. 5.

Disordered $ZrTiO_4$ presents an non-saturated absorption tail in the 2.0–4.0 eV energy range that broadens the absorbance curve of oxides (Fig. 5). Tail formation may be associated with the formation of new electronic levels between the VB and CB promoted by the disordered structure of ZT oxides. The measured gap value decreased from 3.09 to 2.16 eV in the ordered and disordered oxide, respectively, due the formation of new electronic levels between VB and CB [10,13,30,31].

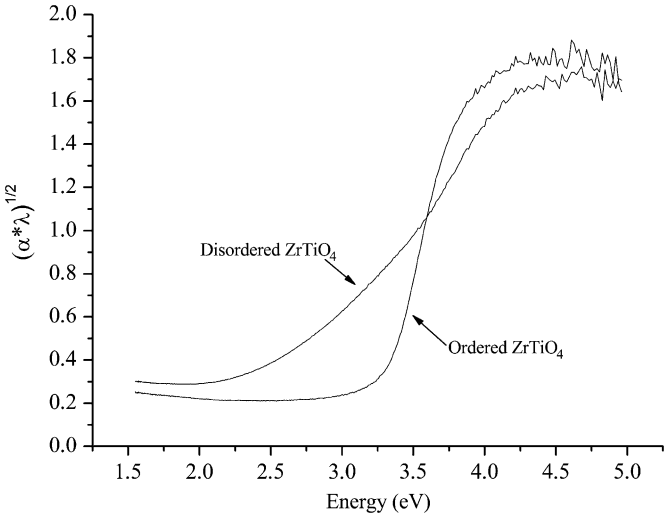

Fig. 5. Spectral UV dependence of $ZrTiO_4$ oxides to the heat treatment temperature (ordered—700 °C and disordered—300 °C).

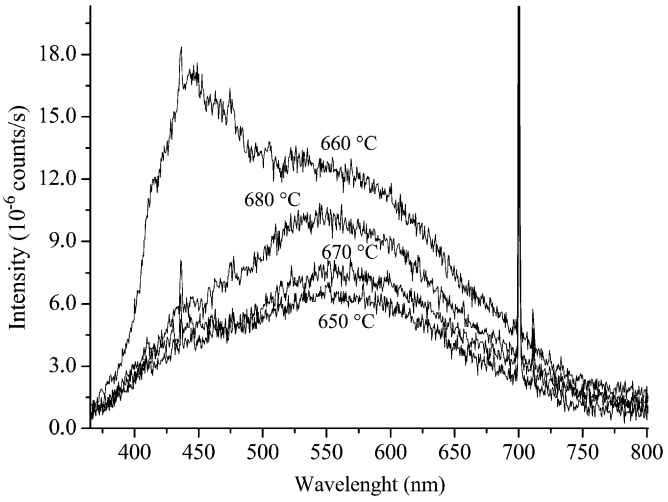

Fig. 7. Photoluminescence in disordered $ZrTiO_4$ treated at 650, 660, 670 and 680 °C.

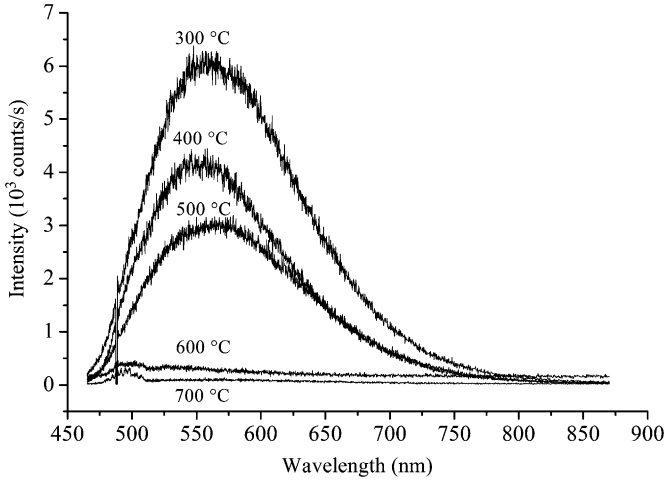

Fig. 6. Photoluminescence in $ZrTiO_4$ powders heat-treated at 400, 500, 600 and 700 °C.

3.4. Photoluminescence

Fig. 6 presents the photoluminescence emission of the ZT powders heat-treated at different temperatures. The powders heated at 300, 400, and 500 °C presented a gradual decrease in the intensity of broad band photoluminescence in the 300–700 nm region. As the temperature increased, the photoluminescence signal decrease until it practically disappeared at 600 °C. A minimal photoluminescent band was detected in the powders treated in temperature range of 650–680 °C (Fig. 7). At 700 °C, where the oxide is in the crystalline phase, the powder displayed no photoluminescence emission. In the photoluminescence spectra displayed in Fig. 6 a weak photoluminescent emission can be observed in the wavelength below 488 nm. Although with low probability, in some absorption/emission processes the energy of the incident photon is lower than the emitted photon energy. In these processes, the first absorption conducts the electrons to some excited levels, where an "extra" energy take the excited electron to levels of higher energy than supplied by laser source. This "extra" energy in our photoluminescence experiments is supplied by the lattice thermal vibration and is equal $k.T$.

According to Xu [19] the increase of long-range order in ZT powders obtained by chemical syntheses are followed by cations' coordination shells exchange from $Ti–O_5$ to $Ti–O_6$ and from $Zr–O_7$ to $Zr–O_6$, yielding ordered ZT in temperatures above 700 °C.

The results presented for the Raman spectroscopy and XRD take us to believe that after to the decomposition of organic precursors the Ti and Zr atoms bond with oxygen atoms yielding $Zr–O_n$ and $Ti–O_n$ clusters with the metal–oxygen distorted bonds and different values of n in relation to crystalline structure. With the temperature increase, the local distortions decrease and the clusters begin to linking in a previous stage of ZT structural definition, in this moment the coordination number of $Ti–O_5$ and $Zr–O_7$ start to change, leading the clusters to a six-fold coordination, diminishing the degree of structural disorder. This degree of disorder have intimate relation with the photoluminescent emission in ZT.

The results of XRD, Raman spectroscopy and the UV–vis all indicate that the photoluminescence emission is associated with the level of structural organization of ZT oxides. A consequence of the presence of $Ti–O_5$ and $Zr–O_7$ in disordered oxides is the formation of a new electronic configuration in the gap region that become viable photoluminescence emission at room temperature [30,32–34].

Thus, photoluminescence is a sensitive probe to detect the crystalline phase formation by variation of structural organization level of ZT oxide. Based on our photoluminescent

results, we are confident that this oxide system presents three levels of self-organization:

(1) *Short-range order*: With the presence of $Ti–O_5$ and $Zr–O_7$ in the oxides treated at 300–600 °C, making possible emission of photoluminescence due to the change in electronic configuration.
(2) *Medium-range order*: In which ZT displays very weak photoluminescence intensity due to the presence of $Zr–O_7$ and $Ti–O_5$ in a quasi-ordered structure, next to the formation of crystalline phase.
(3) *Long-range order*: With the formation of a thermodynamically stable orthorhombic phase, where the ordered structure are present, with titanium and zirconium atoms in six-fold coordination, and the photoluminescence disappears.

In addition, the formation of orthorhombic ZT phase is resulted of a crystallization process induced by local symmetry change in the $Ti–O_n$ and $Zr–O_n$ bonds. Therefore, crystallization peak of DSC is a border between the disordered and ordered phase. Thus, the crystallization process of ZT is a reaction of the structure of this oxide to local symmetry change in the Zr–O and Ti–O bonds in disordered phase, induced by the increase of heat treatment temperature.

4. Conclusions

Ordered and disordered ZT oxides were obtained by polymeric precursor soft-chemical method and disordered powders displayed photoluminescence emission. This emission is associated with structural organization level of chemically prepared ZT oxide system.

Acknowledgments

The authors gratefully acknowledge the financial support of the Brazilian research funding institutions CNPq, CAPES and FAPESP/CEPID (process number: 03/09517-4) and to Prof. Cristiane Villa by the relevant discussions presented in this work.

References

[1] M.E. Lines, A.M. Glass, Principles and Application of Ferroelectrics and Related Materials, Clarendon Press, Oxford, 1977.
[2] I.C. Cosentino, E.N.S. Muccillo, R. Muccillo, F.M. Vichi, J. Sol–Gel Sci. Technol. 37 (2006) 31.
[3] G.F.G. Freitas, E.R. Leite, E. Longo, P.S. Pizani, Appl. Phys. A—Mater. 3 (78) (2004) 355.
[4] S. Yamamoto, M. Kakihana, S. Kato, J. Alloy Compd. 297 (2000) 81.
[5] A. Bianco, M. Paci, R. Freer, J. Eur. Ceram. Soc. 18 (1998) 1235.
[6] A.P.D. Marques, D.M.A. de Melo, C.A. Paskocimas, P.S. Pizani, M.R. Joya, E.R. Leite, E. Longo, J. Solid State Chem. 179 (2006) 671.
[7] M. Kakihana, J. Sol–Gel Sci. Technol. 6 (1996) 5.
[8] E.R. Leite, C.M.G. Sousa, E. Longo, J.A. Varela, Ceram. Int. 21 (1995) 143.
[9] P.S. Pizani, E.R. Leite, F.M. Pontes, E.C. Paris, J.H. Rangel, E.J.H. Lee, E. Longo, P. Delega, J.A. Varela, Appl. Phys. Lett. 77 (2000) 824.
[10] E. Orhan, F.M. Pontes, C.D. Pinheiro, T.M. Boschi, E.R. Leite, P.S. Pizani, A. Beltrán, J. Andrés, J.A. Varela, E. Longo, J. Solid State Chem. 177 (11) (2004) 3879.
[11] E. Orhan, M. Anicete-Santos, M.A.M.A. Maurera, F.M. Pontes, A.G. Souza, J. Andres, A. Beltran, J.A. Varela, P.S. Pizani, C.A. Taft, E. Longo, J. Solid State Chem. 178 (2005) 1284.
[12] I.A. Souza, M.F.C. Gurgel, L.P.S. Santos, M.S. Góes, S. Cava, M. Cilense, I.L.V. Rosa, C.O. Paiva-Santos, E. Longo, Chem. Phys. 322 (2006) 343.
[13] E. Orhan, M. Anicete-Santos, M.A.M.A. Maurera, F.M. Pontes, C.O. Paiva-Santos, A.G. Souza, J.A. Varela, P.S. Pizani, E. Longo, Chem. Phys. 312 (2005) 1.
[14] A.C. Chaves, S.J.G. Lima, R.C.M.U. Araujo, M.A.M.A. Maurera, E. Longo, P.S. Pizani, L.G.P. Simoes, L.E.B. Soledade, A.G. Souza, I.M.G. dos Santos, J. Solid State Chem. 179 (2006) 985.
[15] E.R. Leite, F.M. Pontes, E.C. Paris, C.A. Paskocimas, E.J.H. Lee, E. Longo, P.S. Pizani, J.A. Varela, V. Mastelaro, Adv. Mater. Opt. Electron. 10 (2000) 235.
[16] Y. Park, Y.H. Kim, H.G. Kim, Mater. Sci. Eng. B 40 (1996) 37.
[17] K. Tanabe, Solid Acids and Bases: Their Catalytic Activity, Academic Press, New York, 1970.
[18] R.E. Newnham, J. Am. Ceram. Soc. 50 (1967) 216.
[19] J. Xu, C. lind, A.P. Wilkinson, S. Pattanaik, Chem. Mater. 12 (2000) 3347.
[20] D.G. Barton, M. Shtein, R.D. Wilson, S.L. Soled, E. Iglesia, J. Phys. Chem. B 103 (1999) 630.
[21] D.L. Wood, J. Tauc, Phys. Rev. B 5 (1972) 3144.
[22] R. Christoffersen, P.K. Davies, J. Am. Ceram. Soc. 75 (1992) 563.
[23] Y. Park, H.G. Kim, Phase Transitions 62 (1997) 209.
[24] Y.K. Kim, H.M. Jang, J. Appl. Phys. 89 (2001) 6349.
[25] P.R. de Lucena, I.M.G. dos Santos, O.D. Pessoa-Neto, A.G. Souza, J.A. Varela, E. Longo, J. Alloys Compd. 397 (2005) 255.
[26] B.M. Reddy, P.M. Sreekanth, Y. Yamad, Q. Xu, T. Kobayashi, Appl. Catal. A 228 (2002) 269.
[27] M.A. Krebs, R.A. Condrate Sr., J. Mater. Sci. Lett. 7 (1988) 1327.
[28] F. Azough, R. Freer, J. Petzelt, J. Mater. Sci. 28 (1993) 2273.
[29] J. Petzelt, et al., Phys. Rev. B 64 (2001) 184111.
[30] A.T. de Figueiredo, S. de Lazaro, E. Longo, E.C. Paris, J.A. Varela, M.R. Joya, P.S. Pizani, Chem. Mater. 18 (2006) 2904.
[31] F.M. Pontes, C.D. Pinheiro, E. Longo, E.R. Leite, S.R. deLazaro, J.A. Varela, P.S. Pizani, T.M. Boschi, F. Lanciotti, Mater. Chem. Phys. 78 (2002) 227.
[32] I.A. Souza, A.Z. Simoes, E. Longo, J.A. Varela, P.S. Pizani, Appl. Phys. Lett. 88 (12) (2006) 211911.
[33] M. Anicete-Santos, L.S. Cavalcante, E. Orhan, E.C. Paris, L.G.P. Simoes, M.R. Joya, I.L.V. Rosa, P.R. de Lucena, M.R.M.C. Santos, L.S. Santos-Junior, P.S. Pizani, E.R. Leite, J.A. Varela, E. Longo, Chem. Phys. 316 (2005) 260.
[34] E. Orhan, F.M. Pontes, E.R. Leite, P.S. Pizani, J.A. Varela, E. Longo, Chem. Phys. Chem. 6 (2005) 1530.